

# Telerobot operators can account for varying transmission dynamics in a visuo-haptic object tracking task

Mohit Singhala, *Student Member, IEEE*, and Jeremy D. Brown, *Member, IEEE*

**Abstract**—Humans possess an innate ability to incorporate tools into our body schema to perform a myriad of tasks not possible with our natural limbs. Human-in-the-loop telerobotic systems (HiLTS) are tools that extend human manipulation capabilities to remote and virtual environments. Unlike most hand-held tools, however, HiLTS often possess complex electromechanical architectures that introduce non-trivial transmission dynamics between the robot’s leader and follower, which alter or obfuscate the environment’s dynamics. While considerable research has focused on negating or circumventing these dynamics, it is not well understood how capable human operators are at incorporating these transmission dynamics into their sensorimotor control scheme. To begin answering this question, we recruited N=12 participants to use a novel reconfigurable teleoperator with varying transmission dynamics to perform a visuo-haptic tracking task. Contrary to our original hypothesis, our findings demonstrate that humans can account for substantial differences in teleoperator transmission dynamics and produce the compensatory strategies necessary to adequately control the teleoperator. These findings suggest that advances in transparency algorithms and haptic feedback approaches must be coupled with control designs that leverage the unique capabilities of the human operator in the loop.

## I. INTRODUCTION

The human ability to make and use tools is a key characteristic defining the types of tasks we can perform, and how well we can perform them. From a very early age, we learn to utilize tools to interact with our environment and perform tasks that are difficult to perform with only our natural limbs. For simple mechanical tools, we can incorporate the tool’s actuation dynamics into our motor control scheme [1]–[3]. Thus, we can exploit these dynamics to control our energetic interactions with the environment.

Teleoperators are a special class of tools that are intended to augment human capabilities to overcome challenges associated with distance, scale, and safety. Indeed, for the original teleoperators, such as those developed by Goertz [4], their inherent mechanical architecture and bilateral force-reflecting capabilities allowed for dexterous control over environment interactions in a manner consonant with simpler, less complex, tools. Therefore, it is possible that the actuation dynamics of these mechanical teleoperators too can be incorporated in our motor control scheme in order to accurately control the mechanical energy transmitted to the environment. Despite these benefits, the purely mechanical nature of these teleoperators severely limits their workspace. This shortcoming has been overcome by the inclusion of electromechanical actuation architectures that have catalyzed

Mohit Singhala and Jeremy D Brown are with the Department of Mechanical Engineering, Johns Hopkins University, Baltimore, MD, USA e-mail: mohit.singhala@jhu.edu

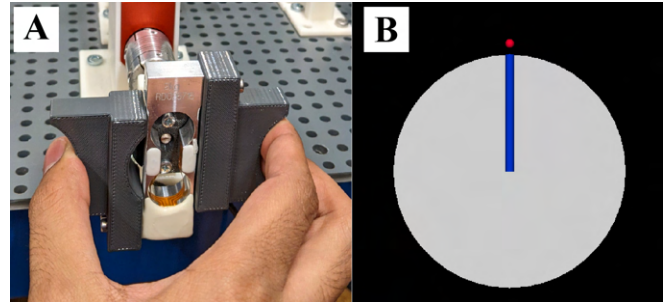


Fig. 1. A) Hand fixture with embedded force sensor; B) Object tracking task virtual environment in which the participant controls the gray disc to track the red target ball.

the development of human-in-the-loop telerobotic systems (HiLTS) [5].

To achieve bilateral force-reflection in modern HiLTS, closed-loop control schemes must be employed to link the mechanical energy input by the operator at the leader side of the telerobot to the mechanical energy output at the follower into the environment. These controllers, however, inherently introduce transmission dynamics between the leader and follower that can significantly alter the energetic interactions between the operator and the environment. Thus, telerobotic transparency has been a topic of considerable research over the last four decades [6]–[9].

Transparency, by definition, requires that the operator’s perceived impedance matches that of the environment being explored through the telerobot [10]. The transmission dynamics introduced by the telerobot’s closed-loop control architecture cannot distort this mechanical energy flow [11], [12]. Given the uncertainty associated with the dynamic state of the operator’s limb(s), as well as the dynamic state of the environment, the pursuit of perfect transparency generally results in a tradeoff between system performance and control stability [11], [13], as perfectly transparent telerobots require infinite stiffness, continuous (non-quantized) sensing, and zero time-delay between the leader and follower. Considering these stability issues, approaches such as passivity have attempted to improve teleoperator stability by monitoring the energy flow in the system [14], [15]. Stable passive controllers, however, often lead to increased damping in the closed-loop dynamics, which decreases the telerobot’s transparency and masks the dynamics of the environment felt by the operator [16]. Thus, true transparency represents a lofty ideal that has yet to be robustly achieved on physical systems.

As an alternative to direct force-reflection, there is a growing body of work evaluating the efficacy of cutaneous sensory substitution feedback as a means of replacing traditional kinesthetic cues [17]–[20]. The benefit of this approach is that it provides haptic information without directly affecting the operator’s control over the telerobot or the closed-loop stability of the human-robot system. To provide utility to the operators, these cutaneous cues need to be easily discernible and discriminable [21]. Likewise, they need to intuitively convey information about environment dynamics, a significant challenge given their non-collocated nature [12].

While passivity and sensory substitution offer significant utility in many scenarios, they are focused primarily on compensating for the transmission dynamics of the telerobot, or bypassing these dynamics all together. It is still, however, not known to what degree the human operator in the telerobotic control loop can account for, or even incorporate these transmission dynamics into their existing control scheme. While limited but promising evidence suggests that this accommodation of tool dynamics extends to teleoperators [21]–[25], it is unclear to what extent different telerobot transmission dynamics impact an operator’s task performance. We utilize a previously developed teleoperator testbed with reconfigurable mechanical and electromechanical transmissions [26] to investigate the effects of transmission dynamics on performance in a visuo-haptic object-tracking task, this manuscript serves as an extension of our prior work. We chose object-tracking because of its relevance to many teleoperation scenarios requiring precise position control. We *hypothesize*, that teleoperator configurations with simpler transmission dynamics will be more easily incorporated by the operator, resulting in superior task performance.

## II. EXPERIMENTAL SETUP

The teleoperation testbed is a reconfigurable 1DoF closed-loop rotational electromechanical device that can be configured into different model teleoperation systems. The testbed consists of three modules: 1) operator interface, 2) reconfigurable teleoperator, 3) Environment. Each teleoperator configuration is achieved by selectively engaging a combination of four different transmissions with a common user input and a common output to the environment. While key features of the teleoperator testbed, relevant to this manuscript are discussed below, complete details of the mechatronic design and evaluation of teleoperator can be found in Singhal and Brown [26].

### A. Module 1: Operator Interface

The operator interface connects the operator to the leader side of the teleoperator. The hand fixture (see Fig. 1A) features a 3D printed open grip hand fixture. The hand fixture consists of two symmetric sections coupled together through an Omega single-point load cell (LC61SP-2KG) to measure grip force. The fixture design includes ridges that allow participants to comfortably hold the fixture with a tripod-style grip using their thumb, index, and middle fingers.

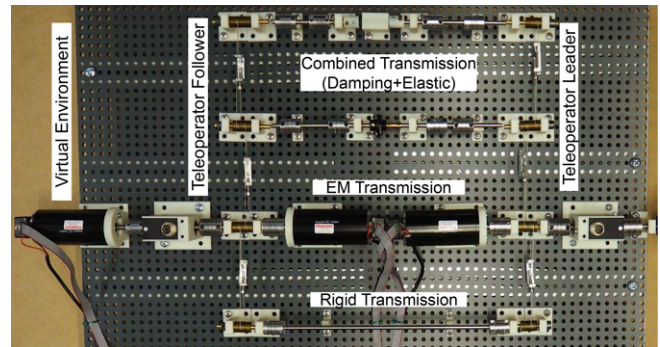


Fig. 2. Reconfigurable teleoperator with four transmissions 1) Rigid, 2) Electromechanical (EM), and 3) Combined (damping + elastic), connected in parallel using capstan drives to a common leader and a common follower. Follower is connected to a motor rendering the virtual environment.

### B. Module 2: Reconfigurable Teleoperator

The reconfigurable teleoperator comprises four separate transmissions in parallel (see Fig. 2). All transmissions are connected via capstan drives and their input shafts rotate in the same direction as the hand fixture in the operator interface module. This allows the four different transmissions to have one common input (leader) and one common output (follower). The different transmissions can be engaged and disengaged independently or simultaneously, to create various teleoperator transmissions with varying dynamics. Each transmission is described below.

- 1) Rigid Mechanical Transmission: A steel shaft mechanically couples the leader and follower of the teleoperator with no torque or position scaling.
- 2) Combined Mechanical Transmission: A bi-directional, gearless, oil-filled rotary damper (9.45 mNm/rad/s) and a bi-directionally compressible Neoprene rod (Shore 80D; 6.3 mm diameter; 50 mm length) mechanically couple the leader and follower of the teleoperator. The damper has a minimum torque rating of 15 mNm. The neoprene rod is enclosed in a 3D printed housing to prevent buckling.
- 3) Electromechanical Transmission: Two direct-drive Maxon RE50 (200 W) motors, each with a 3-channel 500 CPT HEDL encoder electromechanically couples the leader and the follower. The motors can be programmed to enable unilateral and bilateral teleoperation (control laws discussed in Section II-D).

### C. Module 3: Environment

The environment comprises a Maxon RE50 (200W) motor with a 3-channel 500 CPT HEDL encoder that can render virtual environments with a peak torque of 467 mNm and a maximum continuous torque of 233 mNm (see Fig. 2).

### D. Data Acquisition and Control

All three Maxon DC actuators in the testbed are powered by a Quanser AMPAQ L4 linear current amplifier. All data acquisition and control operations are performed with a Quanser

Q8 DAQ running at 1 Khz through a MATLAB/Simulink and QUARC interface on a Dell Precision T5810 workstation.

To generate the bilateral electromechanical transmission (see Section II-B), the leader and follower actuators are coupled in a position-position control architecture with the following proportional-derivative control law:

$$T_l(t) = K_p(\theta_f - \theta_l) + K_d(\dot{\theta}_f - \dot{\theta}_l)$$

$$T_f(t) = K_p(\theta_l - \theta_f) + K_d(\dot{\theta}_l - \dot{\theta}_f)$$

where  $T_l$  is the torque command sent to the leader motor,  $T_f$  is the torque command sent to the follower motor,  $\theta_l/\dot{\theta}_l$  is the angular position/velocity of the leader,  $\theta_f/\dot{\theta}_f$  is the angular position/velocity of the follower,  $K_p$  is the proportional gain (0.1), and  $K_d$  is the derivative gain (0.01). A unilateral architecture can also be rendered by setting  $T_l(t) = 0$ .

### III. METHODS

#### A. Participants

We recruited n=12 individuals (9 female, 3 male) to participate in the study. All participants were college-aged adults attending undergraduate or graduate level engineering programs. All participants provided written informed consent according to a protocol approved by the Johns Hopkins School of Medicine Institutional Review Board (Study# IRB00263386). Participants were compensated at a rate of \$10/hour.

#### B. Study Design

After providing informed consent, participants were seated in front of the teleoperator testbed. Direct view of the testbed was obstructed by an opaque acrylic panel. Participants could, therefore, only see and touch the operator interface of the testbed (see Fig. 3). Participants were instructed to maintain a tripod-style grip on the two halves of the hand fixture with their self-identified dominant hand. A high-definition monitor was placed directly above the panel at eye-level to provide visual feedback and instructional cues.

A within-subjects study design was utilized, wherein each participant performed an object-tracking task (described below) as part of a larger set of object exploration tasks in each of the teleoperator transmission configurations: Rigid Transmission, Combined Transmission, Electromechanical-unilateral, and Electromechanical-bilateral. The order in which participants used each teleoperator configuration was randomized and counterbalanced to control for any learning affects.

#### C. Object-Tracking Task

In this task, participants were instructed to use the teleoperator to track a moving ball displayed on the monitor with a virtual disk (see Fig. 1B). The virtual disk was rendered by the virtual environment motor as being rigidly attached to the follower side of the teleoperator. The virtual disk rotated in a viscoelastic medium with damping and stiffness coefficients of .67 mNm/deg/s and 116.75 mNm/deg, respectively. Due to the inherent inertia of the virtual environment motor, no

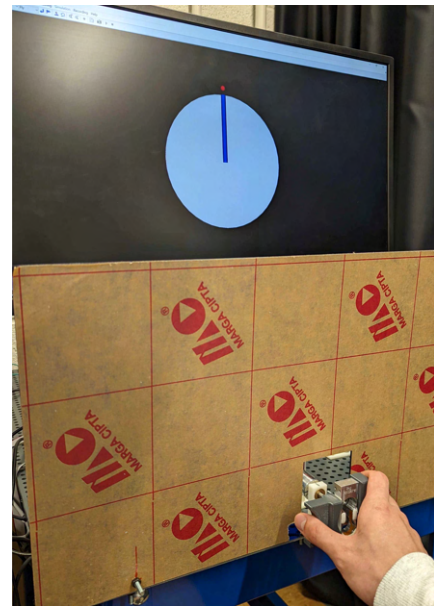


Fig. 3. Participant gripping the hand fixture while looking at the screen displaying the virtual environment.

additional virtual inertia was rendered for the disk. The ball rotated about the same axis as that of the disk and oscillated between  $\pm 45$  degrees, always starting from the zero position.

The task included a training period of nine trials. In each trial, the ball moved for 8 seconds, and the position followed a sinusoidal oscillatory pattern at 0.25Hz, 0.5Hz and 0.75Hz frequencies (rendered separately). Three trials were performed at each frequency, presented randomly. Once the training was complete, participants completed the main tracking task wherein the ball followed a more complex trajectory that included all three principal frequencies in a sum-of-sines oscillatory pattern defined as  $0.4 * \sin(0.25) + 0.25 * \sin(0.5) + 0.55 * \sin(0.75)$  (see Fig. 4). A familiarization phase of approximately 3 minutes was included before each object-tracking block, for each teleoperator, where the participants freely explored environments of different damping and stiffness coefficients, presented randomly, to gain an understanding of how to interact with the teleoperator.

The principal frequencies defining the trajectory of the ball are of the same range as typically seen in fine upper limb motion tasks like surgery [27]. The angular velocities at which the task was performed was informed by our prior work investigating effects of exploration dynamics on perception [28].

The amplitudes for each frequency were chosen heuristically based on pilot studies to achieve a waveform that would require intentional adjustments from the participant to adequately track. Eight tracking trials were performed for each teleoperator configuration, where each trial lasted for 12 seconds and the path of the ball was the same for each trial.

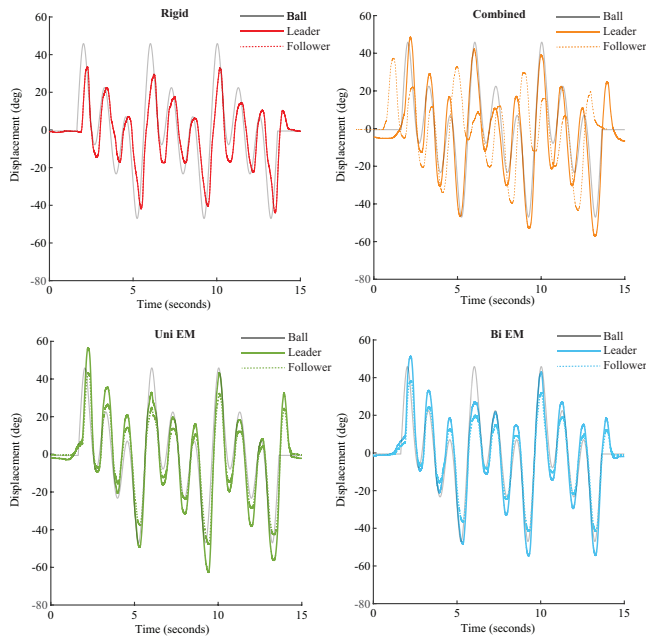


Fig. 4. Visual representation of tracking task trajectory signals. Each plot illustrates the trajectory of the ball for a single trial (black solid trace), average leader displacement (color solid trace) and follower displacement (color and dash trace) of all participants for each teleoperator configuration, averaged over all trials.

#### D. Survey

Participants responded to the following survey questions after the task, for each teleoperator configuration, on a scale of 1 to 5 (Strongly Disagree to Strongly Agree). Participants were also allowed to voluntarily share any general comments after each task.

- 1) I relied on visual feedback for tracking.
- 2) I relied on haptic feedback for tracking.

#### E. Metrics and Statistical Analysis

The following metrics were used to analyze participants' performance in the object-tracking task, and were measured separately for each participant and for each teleoperator configuration.

- 1) Tracking error: Root-mean-squared differences between the angular position of the teleoperator follower and the angular position of the ball.
- 2) Tracking adjustments: Root-mean-squared differences between the angular position of the teleoperator leader (directly controlled by the participant) and the angular position of the ball.
- 3) Grip Force: The mean grip force used by the participant to grip the hand fixture on the operator interface.

Tests for assumptions of normality, outliers, and sphericity were performed as needed for all tests mentioned below. Bonferroni corrections for multiple comparisons were also applied as needed. A two-way repeated measures ANOVA was run to determine the effects of different "teleoperator

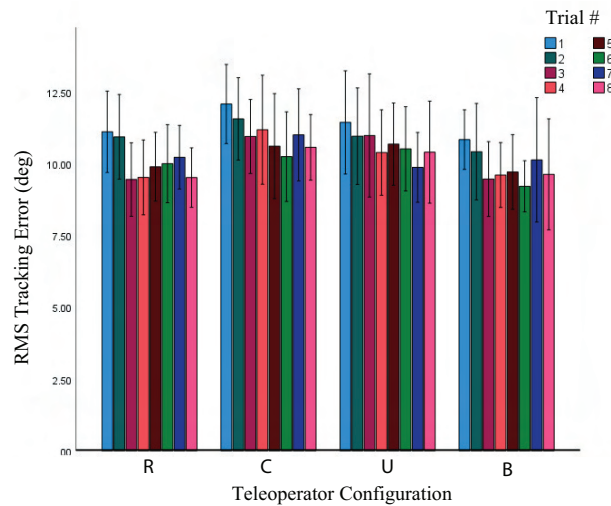


Fig. 5. Mean tracking errors for each trial, for each teleoperator configuration. Please note the general downward trend from first to last trial for all teleoperators. R: rigid transmission, C: combined transmission, U: Electromechanical-unilateral, B: Electromechanical-bilateral. Error bars represent 95% confidence intervals.

configurations" and "trial number" on the tracking error. A separate two-way repeated measures ANOVA was used to determine the effects of different "teleoperator configurations" and "trial number" on the tracking adjustments. A one-way repeated measures ANOVA was used to compare the mean grip force across the four teleoperator configurations. Prefatory descriptive analysis was performed for the survey responses.

## IV. RESULTS

### A. Tracking Error

There were two outliers in the tracking error data, however the values were not unusually large and were not the result of any measurement or system error. Therefore these outliers were not removed from the analysis. The data was normally distributed, as assessed by visual inspection of the normal QQ plot and Kolmogorov-Smirnov test ( $p > 0.05$ ). The assumption of sphericity was met, as assessed by Mauchly's test of sphericity,  $\chi^2(5) = 0.941$ ,  $p = .967$ . There were significant differences in tracking errors based on the trial number,  $F(7,77) = 6.616$ ,  $p < 0.001$ , partial  $\eta^2 = .376$  (see Fig. 5). Post hoc analysis with a Bonferroni correction revealed statistically significant comparisons. The primary comparison of interest is the difference in tracking performance between first and last trial (trial eight). The tracking error in the first trial was found to be significantly higher compared to the eighth trial (1.34 (95% CI, 0.09 to 2.58) deg,  $p = 0.031$ ).

No statistically significant differences were found in participants' tracking errors between the different teleoperator configurations,  $F(3,33) = 1.189$ ,  $p < 0.329$ , partial  $\eta^2 = .098$  (see Fig. 6). No statistically significant interaction effects were found between trial number and teleoperator configuration  $p > 0.05$ .

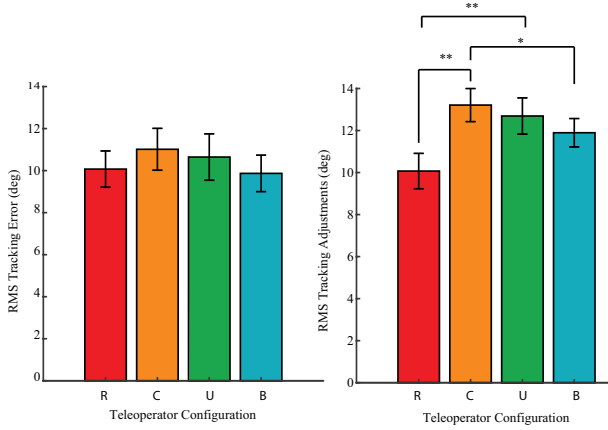


Fig. 6. Mean tracking error for each teleoperator (left) and mean tracking adjustment values (right). R: rigid transmission, C: combined transmission, U: Electromechanical-unilateral, B: Electromechanical-bilateral. Error bars represent 1 standard deviation.

### B. Tracking adjustments

There were no outliers in the tracking adjustments data. The data was normally distributed, as assessed by visual inspection of the normal QQ plot and Kolmogorov-Smirnov test ( $p > 0.05$ ). The assumption of sphericity was met, as assessed by Mauchly's test of sphericity,  $\chi^2(5) = 3.225$ ,  $p = .667$ . There were significant differences in tracking adjustments made by participants between the different teleoperator configurations,  $F(3,33) = 12.64$ ,  $p < 0.001$ , partial  $\eta^2 = .54$  (see Fig. 6). Post hoc analysis with a Bonferroni correction revealed statistical significant differences in root-mean-squared displacement between the leader and the ball for the following teleoperator configuration pairs:

- Greater tracking adjustments (i.e., larger differences between the leader and the ball) were made with the combined teleoperator compared to the rigid teleoperator (3.14 (95% CI, 1.15 to 5.13) deg,  $p = 0.002$ )
- Greater tracking adjustments were made with electromechanical-unilateral teleoperator compared to the rigid teleoperator (2.62 (95% CI, 1.06 to 4.08) deg,  $p = 0.001$ )
- Greater tracking adjustment were made with the combined teleoperator compared to the electromechanical-bilateral teleoperator (1.32 (95% CI, 0.11 to 2.63) deg,  $p = 0.048$ )

We found no main effects from trial number or interaction effects between trial number and teleoperator configuration  $p > 0.05$ .

### C. Grip force

There were no outliers in the grip force data. The data was normally distributed, as assessed by visual inspection of the normal QQ plot and Kolmogorov-Smirnov test ( $p > 0.05$ ). The assumption of sphericity was not met, as assessed by Mauchly's test of sphericity,  $\chi^2(5) = 12.99$ ,  $p = .024$ . Therefore, a Greenhouse-Geisser correction was applied ( $\epsilon = 0.566$ ).

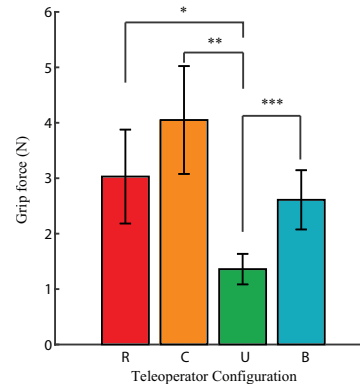


Fig. 7. Mean grip force in Newtons for each teleoperator, for the tracking task. R: rigid transmission, C: combined transmission, U: Electromechanical-unilateral, B: Electromechanical-bilateral. Error bars represent 1 standard deviation.

There were significant differences in the grip force used by participants for the different teleoperator configurations,  $F(1.698, 18.677) = 13.686$ ,  $p < 0.001$ , partial  $\eta^2 = .554$  (see Fig. 7). Post hoc analysis with a Bonferroni correction revealed statistically significant differences in participants' grip force for the following teleoperator pairs:

- Grip force was higher for the rigid teleoperator compared to the electromechanical-unilateral teleoperator (1.67 (95% CI, 0.32 to 3.02) N,  $p = 0.013$ )
- Grip force was higher for the combined teleoperator compared to the electromechanical-unilateral teleoperator (2.69 (95% CI, 0.87 to 4.49) N,  $p = 0.004$ )
- Grip force was higher for the electromechanical-bilateral teleoperator compared to the electromechanical-unilateral teleoperator (1.25 (95% CI, 0.56 to 1.93) N,  $p < 0.001$ )

### D. Survey

Participants reported a higher reliance on visual feedback compared to haptic feedback for all teleoperators configuration. The mean response values for reliance on visual feedback were in the range of 4.67 to 4.92 for all teleoperators, indicating a strong agreement. The mean response value for reliance on haptic feedback were in the range of 2.08 to 2.75, indicating a moderate disagreement, with lowest reliance value reported for unilateral electromechanical teleoperator. Figure 8 shows a visualization of these results.

## V. DISCUSSION

In this manuscript, we investigated the impact of teleoperator transmission dynamics on operator task performance. Using a novel teleoperator testbed that featured four interchangeable teleoperator transmissions, we asked participants to perform a visuo-haptic object-tracking task with each teleoperator variant. In our experiment, task performance metrics measured the degree to which participants were able to accurately track the object, and the compensatory control strategies participants adopted in their pursuit of perfect tracking. While we hypothesized that configurations with

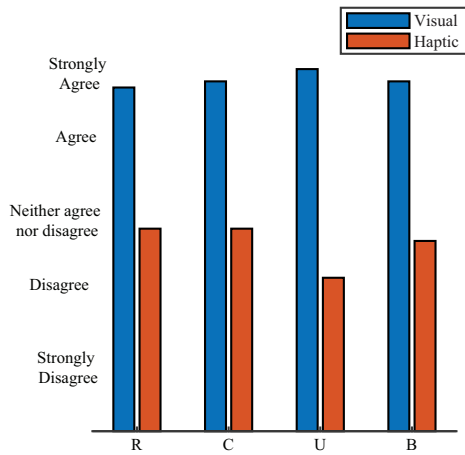


Fig. 8. Mean scores from the survey to Q1. I relied on visual feedback for tracking (blue) and Q2. I relied on haptic feedback for tracking, for the four teleoperator configurations in the order: R: rigid transmission, C: combined transmission, U: Electromechanical-unilateral, B: Electromechanical-bilateral.

simpler dynamics (e.g., rigid transmission) would result in superior performance, our results highlight an interesting and somewhat unexpected finding. We observed no significant differences in tracking performance between the different teleoperator configurations. At the same time, however, we did find that participants used significantly different compensatory strategies to achieve similar performance in each teleoperator configuration.

Most surprising in our results, was the finding that the rigid teleoperator configuration, which has often been referred to as the “gold standard,” did not lead to significantly better performance than any of the other three teleoperator configurations. This configuration featured a rigid connection between the leader and follower that allowed for a one-to-one torque and position mapping. The other three teleoperators, however, featured mechanisms (mechanical or electromechanical) that introduced delays and varying amounts of position or torque scaling between the operator and the virtual disk. Therefore, in order to accurately perform the tracking task, participants had to account for these dynamics as they rotated the hand fixture. This is reflected in our results as we found significant differences across the teleoperator configurations in terms of the tracking adjustments participants made on the leader end of the teleoperator to produce a given output on the teleoperator follower.

Our finding of differences in tracking adjustments, along with observations that participants significantly improved their performance as the experiment progressed, lends support to the theory that humans can model their tools separately from the environment, and that these models are updated with more experience [29]–[32]. Generally, this ability to invert and incorporate a tool’s dynamics is limited to tools with simple dynamics [33]. However, the extension of this behavior to continuous use of tools with complex dynamics, such as the teleoperators used in this experiment, can have

significant implications on how we think about the human operator in the teleoperator control loop.

Adding further support to our argument that participants were likely inverting the teleoperator dynamics is our finding that our participants used smaller grip forces when using the unilateral (no force-reflection) electromechanical teleoperator compared to all other teleoperators. This observation conforms to the theory that humans match their limb impedance to the impedance of their tool [34]. Since the unilateral electromechanical teleoperator does not produce haptic feedback, it offers the lowest impedance to the operator’s actions.

Our quantitative task performance findings are also substantiated by participants’ qualitative response. In particular, participants reported a higher reliance on visual feedback to complete the task. While visual dominance is expected in a visuo-haptic tracking task, it seems as though participants negated the haptic feedback; on average, participants disagreed with the statement that they found haptic feedback to be useful for either of the two electromechanical teleoperators. It is therefore possible that participants are learning to invert the model of the teleoperator (and incorporate the teleoperator’s dynamics) based largely on visual observation. This likely explains why performance with the rigid teleoperator does not lead to superior tracking than the other three teleoperators, nor why the bilateral electromechanical teleoperator does not lead to superior performance than the unilateral variant. It is worth reiterating here that the virtual disk participants were controlling had second-order dynamics resulting from the virtual environment motor inertia and the rendered visco-elastic environment.

While our results can inform a wide variety of teleoperation research and applications, we acknowledge that at present, any inferences drawn from this study are likely task and system dependent. Though not representative of all telerobotic tasks, object tracking is a common task in teleoperation and is used extensively in haptic-feedback research. For tasks that require higher frequency motion, or tasks where environment perception is of primary importance, these results may vary. Likewise, different system parameters will likely lead to different compensatory strategies. There also exist systems for which no amount of compensation would lead to equivalent performance (e.g.,  $K_p=K_d=0$ , for the electromechanical teleoperator). Still, the present study represents a first of its kind robust and equitable comparison of four distinct teleoperator configurations, with results demonstrating the need to reconsider the human operator in the telerobotic control loop. Future studies with this testbed will focus on a variety of task performance and perceptual investigations. In addition, this testbed and its associated tasks can be used to investigate the role of internal models and tool embodiment in motor control.

#### ACKNOWLEDGMENT

This material is based upon work supported by the National Science Foundation under NSF Grant #1910939.

## REFERENCES

- [1] A. Farnè and E. Làdavas, "Dynamic size-change of hand peripersonal space following tool use," *NeuroReport*, 2000.
- [2] A. Maravita and A. Iriki, "Tools for the body (schema)," *Trends in Cognitive Sciences*, vol. 8, no. 2, pp. 79–86, 2004.
- [3] A. Iriki, M. Tanaka, and Y. Iwamura, "Coding of modified body schema during tool use by macaque postcentral neurones," *NeuroReport*, vol. 7, no. 14, pp. 2325–2330, 1996.
- [4] R. C. Goertz, "Mechanical master-slave manipulator," *Nucleonics*, vol. 12, no. 11, pp. 45–46, 1954.
- [5] R. C. Goertz, , and F. Bevilacqua, "A Force-Reflecting Positional Servomechanism," *Nucleonics*, vol. 10, no. 11, pp. 43–45, 1952.
- [6] D. A. Lawrence, "Stability and Transparency in Bilateral Teleoperation," *IEEE Transactions on Robotics and Automation*, vol. 9, no. 5, pp. 624–637, 1993.
- [7] K. Hashtrudi-Zaad and S. E. Salcudean, "Analysis of control architectures for teleoperation systems with impedance/admittance master and slave manipulators," *International Journal of Robotics Research*, vol. 20, no. 6, pp. 419–445, 2001.
- [8] G. Niemeyer, C. Preusche, S. Stramigioli, and D. Lee, "Telerobotics," *Springer Handbook of Robotics*, pp. 1087–1108, 1 2016.
- [9] M. Tavakoli, R. V. Patel, R. V. Moallem, and A. Aziminejad, *Haptics for teleoperated surgical robotic systems*, 2008.
- [10] S. E. Salcudean, M. Zhu, W. H. Zhu, and K. Hashtrudi-Zaad, "Transparent bilateral teleoperation under position and rate control," *International Journal of Robotics Research*, vol. 19, no. 12, pp. 1185–1202, 2000.
- [11] N. Hogan, "Controlling impedance at the man/machine interface," in *Proceedings, 1989 International Conference on Robotics and Automation*, 1989, pp. 1626–1631.
- [12] J. D. Brown, M. K. Shelley, D. Gardner, E. A. Gansallo, and R. B. Gillespie, "Non-Colocated Kinesthetic Display Limits Compliance Discrimination in the Absence of Terminal Force Cues," *IEEE Transactions on Haptics*, vol. 9, no. 3, pp. 387–396, 2016.
- [13] R. J. Adams and B. Hannaford, "Stable haptic interaction with virtual environments," *IEEE Transactions on Robotics and Automation*, vol. 15, no. 3, pp. 465–474, 1999.
- [14] J. J. Abbott and A. M. Okamura, "Effects of position quantization and sampling rate on virtual-wall passivity," *IEEE Transactions on Robotics*, vol. 21, no. 5, pp. 952–964, 2005.
- [15] J. E. Colgate and G. G. Schenkel, "Passivity of a class of sampled-data systems: Application to haptic interfaces," *Journal of Robotic Systems*, 1997.
- [16] N. Colonnese and A. M. Okamura, "Analysis of effective impedance transmitted to the operator in position-exchange bilateral teleoperation," *2017 IEEE World Haptics Conference, WHC 2017*, pp. 328–333, 2017.
- [17] N. Thomas, G. Ung, C. McGarvey, and J. D. Brown, "Comparison of vibrotactile and joint-torque feedback in a myoelectric upper-limb prosthesis," *Journal of NeuroEngineering and Rehabilitation*, vol. 16, no. 1, 2019.
- [18] C. Pacchierotti, L. Meli, F. Chinello, M. Malvezzi, and D. Prattichizzo, "Cutaneous haptic feedback to ensure the stability of robotic teleoperation systems," *International Journal of Robotics Research*, vol. 61, no. 20, pp. 1773–1787, 2015.
- [19] C. Pacchierotti, D. Prattichizzo, and K. J. Kuchenbecker, "Cutaneous feedback of fingertip deformation and vibration for palpation in robotic surgery," *IEEE Transactions on Biomedical Engineering*, vol. 63, no. 2, pp. 278–287, 2016.
- [20] J. D. Brown, J. N. Fernandez, S. P. Cohen, and K. J. Kuchenbecker, "A wrist-squeezing force-feedback system for robotic surgery training," in *2017 IEEE World Haptics Conference, WHC 2017*, 2017, pp. 107–112.
- [21] J. W. Sensinger and S. Dosen, "A Review of Sensory Feedback in Upper-Limb Prostheses From the Perspective of Human Motor Control," 2020.
- [22] M. Markovic, M. A. Schweisfurth, L. F. Engels, T. Bentz, D. Wüstefeld, D. Farina, and S. Dosen, "The clinical relevance of advanced artificial feedback in the control of a multi-functional myoelectric prosthesis," *Journal of NeuroEngineering and Rehabilitation*, vol. 15, no. 28, 2018.
- [23] M. Štrbac, M. Isaković, M. Belić, I. Popović, I. Simanić, D. Farina, T. Keller, and S. Došen, "Short-and long-term learning of feedforward control of a myoelectric prosthesis with sensory feedback by amputees," *IEEE Transactions on Neural Systems and Rehabilitation Engineering*, vol. 25, no. 11, pp. 2133–2145, 2017.
- [24] I. Nisky, A. M. Okamura, and M. H. Hsieh, "Effects of robotic manipulators on movements of novices and surgeons," *Surgical Endoscopy*, vol. 28, no. 7, pp. 2145–2158, 2014.
- [25] I. Nisky, M. H. Hsieh, and A. M. Okamura, "Uncontrolled manifold analysis of arm joint angle variability during robotic teleoperation and freehand movement of surgeons and novices," *IEEE Transactions on Biomedical Engineering*, vol. 61, no. 12, pp. 2869–2881, 2014.
- [26] M. Singhal and J. D. Brown, "A novel testbed for investigating the impact of teleoperator dynamics on perceived environment dynamics," in *2021 IEEE/RSJ International Conference on Intelligent Robots and Systems (IROS)*, 2021, pp. 8358–8364.
- [27] C. N. Riviere, R. S. Rader, and P. K. Khosla, "Characteristics of hand motion of eye surgeons," in *19th Annual International Conference of the IEEE Engineering in Medicine and Biology Society. 'Magnificent Milestones and Emerging Opportunities in Medical Engineering' (Cat. No.97CH36136)*, vol. 4, 1997, pp. 1690–1693.
- [28] M. Singhal and J. D. Brown, "Prefatory study of the effects of exploration dynamics on stiffness perception," in *IEEE Haptics Symposium, HAPTICS*, vol. 2020-March, 2020, pp. 128–133.
- [29] L. Cardinali, F. Frassinetti, C. Brozzoli, C. Urquizar, A. C. Roy, and A. Farnè, "Tool-use induces morphological updating of the body schema," *Current Biology*, vol. 19, no. 12, p. 1157, 2009.
- [30] M. Martel, L. Cardinali, A. C. Roy, and A. Farnè, "Tool-use: An open window into body representation and its plasticity," *Cognitive Neuropsychology*, vol. 33, no. 1-2, pp. 82–101, 2016.
- [31] C. Nabeshima, Y. Kuniyoshi, and M. A. Lungarella, "Adaptive body schema for robotic tool-use," *Advanced Robotics*, vol. 20, no. 10, pp. 1105–1126, 2006.
- [32] V. U. Weser and D. R. Proffitt, "Expertise in Tool Use Promotes Tool Embodiment," *Topics in Cognitive Science*, vol. 13, no. 4, pp. 597–609, 2021.
- [33] A. Maravita and A. Iriki, "Tools for the body (schema)," 2004.
- [34] M. A. Krutky, V. J. Ravichandran, R. D. Trumbower, and E. J. Perreault, "Interactions between limb and environmental mechanics influence stretch reflex sensitivity in the human arm," *Journal of Neurophysiology*, vol. 103, no. 1, pp. 429–440, 2010.